National Physical Laboratory

NPL REPORT MAT 84

ELECTROCHEMICAL POLARISATION MEASUREMENTS ON A 12Cr MARTENSITIC STAINLESS STEEL IN DILUTE NACL

L. GUO, S. ZHOU AND A. TURNBULL

NOVEMBER 2016

Department for Business, Energy & Industrial Strategy

FUNDED BY BEIS

Electrochemical polarisation measurements on a 12Cr martensitic stainless steel in dilute NaCl

Liya Guo, Shengqi Zhou and Alan Turnbull
Materials Division

ABSTRACT

Electrochemical polarisation tests were carried out to provide input data to the model of crack chemistry being developed for a 12Cr martensitic stainless steel (FV566) in simulated steam turbine solutions. Potentiodynamic tests with two sweep rates and potentiostatic tests were used to characterise the passive current density of FV566 in neutral NaCl solution at 90 °C with chloride ion concentration of 1000 ppm. The method chosen affected the passive current density obtained. Expressions were obtained for the water reduction kinetics in deaerated neutral solutions and for hydrogen ion reduction kinetics in deaerated acidic solutions of varying pH. The depassivation pH of FV566, measured in deaerated solutions with ~2000 ppm Cl^-, was found to be between 1.7 and 1.9.

ISSN 1754-2979

National Physical Laboratory
Hampton Road, Teddington, Middlesex, TW11 0LW

Approved on behalf of NPLML by Prof. Mark Gee,
Knowledge Leader, Materials Division.

CONTENTS

1 INTRODUCTION

Environmentally assisted cracking of steam turbine blades is a concern in the power industry. The development of the damage is often characterised as: crack precursor development in the form of corrosion pits, transition to crack, small crack growth and long crack growth [1, 2]. The growth rate of long cracks is relatively well characterised and there are sufficient data to support inspection planning and assessment. In service, the development of the small cracks constitutes a significant fraction of the life of the metallic component but the growth rate is less well characterised and has posed challenges in measurement. Recent research at NPL [2-4] has focused on corrosion fatigue and stress corrosion crack growth rate measurements in the small crack regime in simulated steam condensates under normal and upset operating conditions. Modelling of crack chemistry in simulated steam turbine condensate solution is being developed to provide a scientific framework to rationalise and predict the complex effect of operational variables on crack growth rates. However, there is a dearth of relevant electrochemical data required for input parameters. The purpose of this study is to provide such electrochemical data specific to the 12Cr martensitic stainless steels commonly used for blade material. In particular, the passive current density, water reduction kinetics, hydrogen ion reduction kinetics in deaerated acidic solutions and the depassivation pH were characterised.

2 EXPERIMENTAL

2.1 SAMPLE PREPARATION

The test material was FV566, which is commonly used for steam turbine blades and formed the basis of the NPL testing programme [5]. The composition of FV566 is shown in Table 1. Cylindrical test specimens were cut from rectangular bar supplied by Siemens. To minimise the occurrence of crevice corrosion, the specimens were immersed in nitric acid solution (20% by mass) at 50 °C for 2 hours. Afterwards, a nickel wire was spot welded to the specimen. Then the whole specimen, except for the front face, was mounted in 3M™ Scotch-Weld™ structural Epoxy Adhesive EC-9323 B/A. Before the test, the exposed surface of the specimen (1 cm in diameter) was ground to 600 grit and the specimen left overnight in a desiccator cabinet with dry silica beads.

Table 1: Composition of FV566 steel (in mass %).

Steel	**C**	**Si**	**Mn**	**P**	**S**	**Cr**	**Mo**	**Ni**	**V**	**N_b**	**Fe**
Composition	0.12	0.30	0.86	0.013	0.002	11.73	1.64	2.59	0.28	0.13	Bal

2.2 EXPERIMENTAL SET-UP

The set-up of the test is shown in Figure 1. The challenge is to maintain control of water chemistry and temperature at the test temperature of 90 °C, this temperature being typical of the temperature of first condensation on a low pressure turbine and the temperature adopted in our environmentally assisted cracking tests.

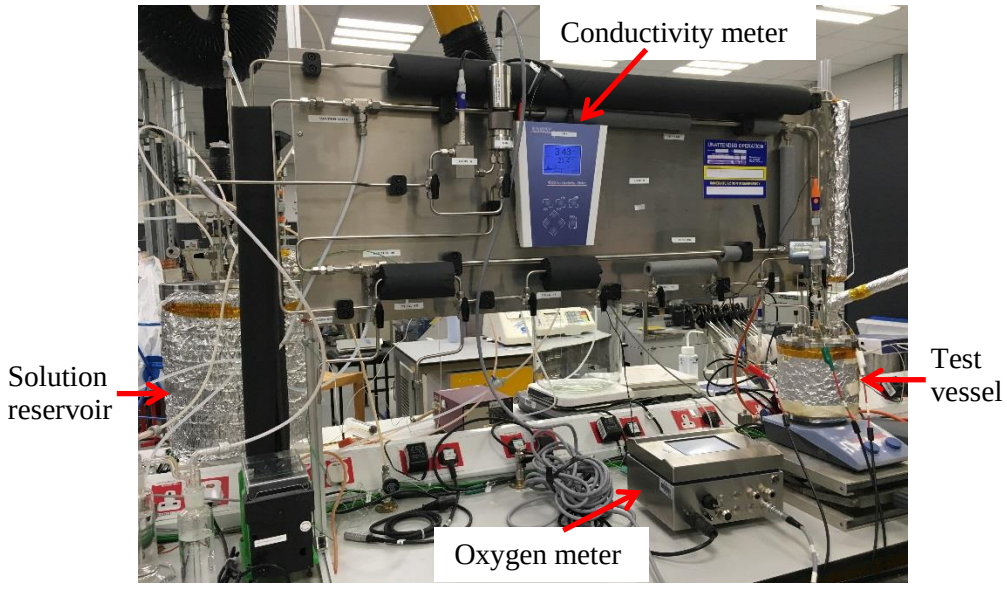

Figure 1: Experimental set-up.

The (~30 L) solution reservoir was filled with at least 22 L of solution. The neutral solution (pH was expected to be 6.2 at 90 °C [6]) was made by dissolving NaCl in deionised water to the required chloride ion concentration, typically 1000 ppm. 1000 ppm Cl^- was chosen primarily to avoid problems of localised attack that might otherwise prevail at higher concentrations, yet still be reasonably conductive, and because it would be close to the value anticipated in a crack when the bulk concentration is near normal water chemistry in a turbine condensate (about 300 ppb Cl^-). To study the hydrogen ion reduction kinetics, the acidic solutions were made by dissolving NaCl and adding controlled amounts of 0.37% HCl or 37% HCl in deionised water to obtain a solution with the desired value of pH at constant chloride ion concentration of 1000 ppm. To determine the depassivation pH of FV566 at 90 °C, a deaerated solution containing 1000 ppm Cl^- with an initial pH of 4.0 was used. The pH of the solution was decreased progressively to 3.0, 2.8, 2.6, 2.3, 2.1, 1.9 and 1.7 by adding 3.7% HCl. With the addition of HCl in this test the chloride ion level in the solution inherently increased. It should be noted that immersion history of the specimen tested under each pH value was different and this might have an effect on the result obtained. Table 2 shows the values of pH and the corresponding concentration of chloride ions of the solutions tested. The pH of the solutions was measured by a pH meter (Jenway 350, calibrated against buffer solutions of pH 2.0, 4.0 and 7.0) at room temperature. For each solution, there was no significant change of the pH values before and after the test.

Table 2: pH values and the corresponding concentration of chloride ions of the solutions used to evaluate the depassivation pH.

Solution	**pH**	**[Cl^-] (ppm)**
1	4.0	1000
2	3.0	1040
3	2.8	1060
4	2.6	1110
5	2.3	1080
6	2.1	1350
7	1.9	1700
8	1.7	2120

The solution in the reservoir was deaerated before and throughout the test by purging nitrogen (N_2) through the solutions. After initial deaeration, solution was circulated from the solution reservoir to the previously deaerated test vessel and recirculation maintained throughout the test. During the test, the

dissolved oxygen (O_2) concentration in the solution was monitored by an oxygen meter (Orbisphere 410) and the conductivity of the solution was monitored by a conductivity meter (Jenway 4520). The O_2 level was below 10 ppb throughout the test and the change in conductivity of the solution before and after the test was within 2%. Apart from recirculation flow, stirring of the solution with a magnetic stirrer at 1000 rpm was undertaken. Five to six specimens were immersed in the test vessel in each test. All tests were carried out at 90 °C.

2.3 ELECTROCHEMICAL TEST PROCEDURE

Measurement of the passive current density of the specimen in the neutral solutions was carried out by two methods. In the potentiodynamic method, specimens were immersed in the deaerated solution at open circuit potential (OCP) for three or four days, followed by an electrode potential sweep from -800 mV (SCE) to the anodic region at 1 mV/min or 10 mV/min. The test was stopped when the current was greater than 10^{-4} A/cm^2. In the potentiostatic method, the specimen was immersed in the deaerated solution at OCP for five days, followed by a potential hold at -300 mV (SCE) for 116 hours to measure the passive current density. -300 mV (SCE) was chosen since it is close to the mean potential value in the passive range.

To measure the water reduction kinetics in neutral solutions the specimen was immersed in the deaerated solution at OCP for eleven days and the electrode potential then swept from -550 mV (SCE), just above OCP, to -1000 mV (SCE) at 1 mV/min. A long immersion time was chosen to have a low passive current to minimise the impact on the net current in the cathodic region.

Determination of the hydrogen ion reduction kinetics was undertaken in acidic solution (1000 ppm Cl^-) in the range pH 2 to pH 4. Specimens were immersed initially in the test solution at OCP for one day (pH 2.2 and pH 4) and three days (pH 3.1). The specimen was held at a potential of -290 mV (SCE) or -300 mV (SCE) for at least 6 hours to obtain a quasi-stable passive oxide. A cathodic polarisation sweep was then commenced from this potential at a sweep rate of 1 mV/min to generate the hydrogen ion reduction polarisation curve.

In the tests to determine the depassivation pH, six specimens were immersed in a solution of 1000 ppm Cl^- at initial pH 4 at OCP for three days. The potential was then swept from OCP to at least 100 mV above the OCP at 1 mV/min to assess whether the metal was passive. If the metal was still passive, i.e. the current did not increase with increasing potential when the potential was at least 100 mV above OCP, 3.7% HCl was added to the solution reservoir to achieve the required value of pH. This was followed by a potential sweep test to evaluate the passive or active state of the specimen. The addition of HCl to lower the value of pH and the following potentiodynamic test was repeated until the metal became active, i.e. the current kept increasing with increasing potential and the current density was greater than 10^{-3} A/cm^2. The immersion time of specimens in solutions at OCP before sweep tests was: 3 days for pH 4 and pH 3; 4 days for pH 2.8; 5 days for pH 2.6 and pH 2.3; 6 days for pH 2.1 and pH 1.9 and 7 days for pH 1.7. A different specimen was used each time except that the same specimen was used at both pH 4 and pH 1.9 and another specimen was tested at both pH 2.6 and pH 1.7 since specimens remained passive at pH 4 and pH 2.6.

All electrochemical tests were carried out with ACM Instrument Gill AC potentiostats.

3 RESULTS AND DISCUSSION

3.1 PASSIVE CURRENT DENSITY

Figure 2 shows the current response of four specimens that were anodically polarised from -800 mV (SCE) at a sweep rate of 1 mV/min or 10 mV/min in deaerated solution containing 1000 ppm Cl^- at 90 °C. A current plateau in the anodic curve, which indicated the passive region, was observed for each test. The passive region was usually followed by a sudden current increase, which indicated pitting corrosion. Crevice corrosion may have occurred in Test 1 with a sweep rate of 1 mV/min since there

were several gradual increases and drops in current after the passive region, unlike the other three tests. However, examination of the specimen surface after testing did not indicate obvious crevice corrosion.

The properties of the passive film are affected by several factors, such as the applied potential [7] and the polarisation time for film formation [8, 9].With a sweep rate of 1mV/min, the passive current density was in the range 0.6-3.1 μA/cm^2. With a sweep rate of 10 mV/min, the passive current density was in the range 3.0–6.5 μA/cm^2. The immersion time of the specimen with a slow sweep rate is greater than that with a fast sweep rate. The greater immersion time might lead to a thicker/denser passive film and consequently lower passive current density [9].

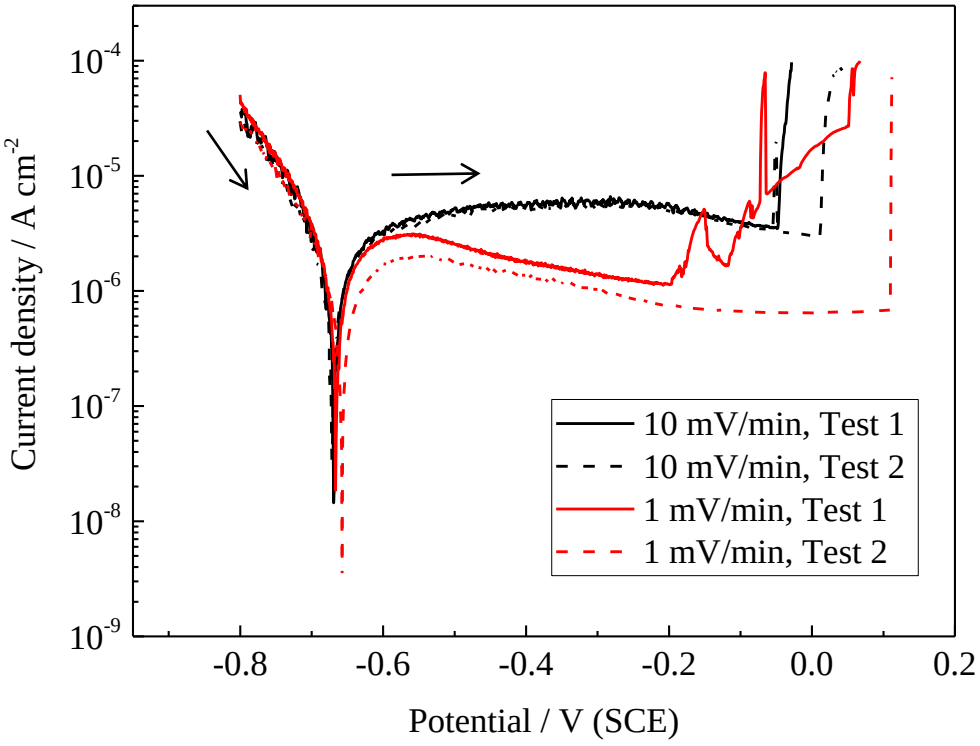

Figure 2: Potential sweeps from cathodic region to anodic region at a sweep rate as indicated in the diagram. The specimens were immersed in the deaerated solution for three days (tests with 10 mV/min and Test 1 with 1 mV/min) and four days (Test 2 with 1 mV/min) before the potential sweep. Tests were carried out in deaerated neutral solutions containing 1000 ppm Cl^- at 90 °C.

Potentiostatic tests were also carried out to study the passive current density of FV566 in neutral solutions. Compared with potentiodynamic tests, potentiostatic tests are more time consuming. However, they give a better characterisation of the quasi-steady-state passive film. Figure 3 illustrates the current decay of a specimen which was immersed in the neutral solution at -300 mV (SCE) for 116 hours. At the beginning of the potentiostatic test, the passive current density was ~19 μA/cm^2, but it decreased rapidly to ~6.1 μA/cm^2 after 11 minutes. The passive current density continued to decrease with time and did not reach a steady state even after an immersion time of 116 hours. The passive current density of the specimen after 116 hours immersion was 0.07 μA/cm^2. The passive current density measured after long-time immersion, as shown in Figure 3, was lower than that obtained from the sweep test (Figure 2). This might be due to the formation of a thicker and denser passive layer during the long-time immersion, as discussed previously.

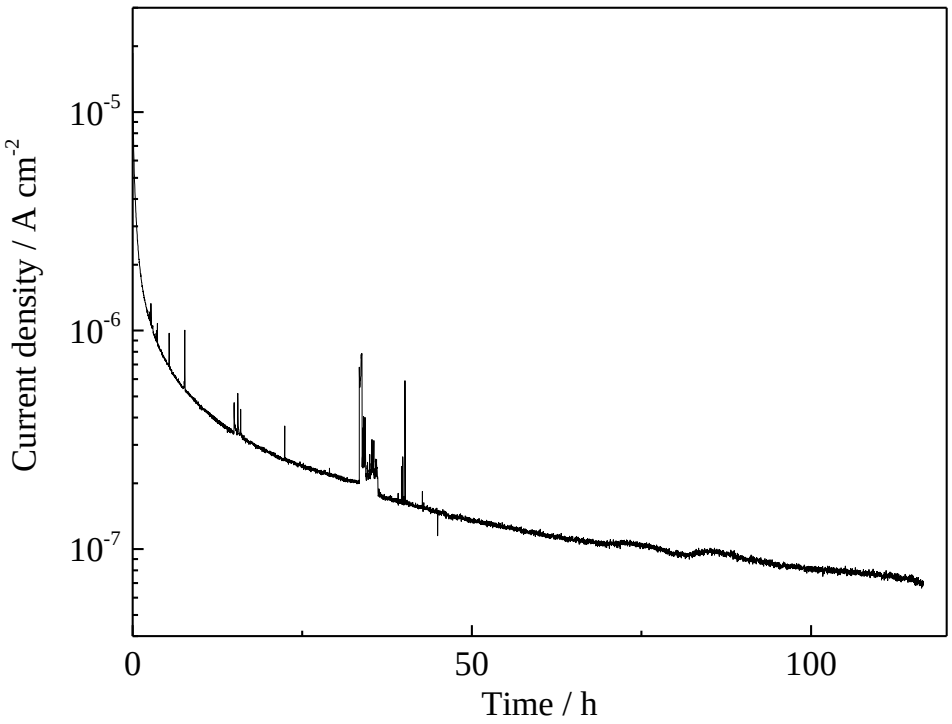

Figure 3: The specimen was held at -300 mV (SCE) for 116 hours in deaerated neutral solutions containing 1000 ppm Cl^- at 90 °C. The potential control was interrupted very briefly at 45 hours and almost immediately restarted with little perturbation of the decay profile. The specimen was immersed in the deaerated solution at OCP for five days before the potentiostatic control.

3.2 WATER REDUCTION KINETICS IN DEAERATED NEUTRAL SOLUTIONS CONTAINING 1000 PPM Cl^- AT 90 °C

Figure 4 shows the current response with the potential sweep from the anodic to cathodic region in deaerated neutral solution containing 1000 ppm Cl^- at 90 °C. In the deaerated neutral solution, water reduction is the dominant reaction in the cathodic region shown in Figure 4. The water reduction reaction occurs as follows [10]:

$$2H_2O + 2e^- \rightarrow H_2 + 2OH^- \quad \textbf{(1)}$$

According to the data in Figure 4, the water reduction kinetics can be represented by:

$$i_{H_2O} = 2.9 \times 10^{-11} \exp\left(-\frac{0.54FE}{RT}\right) \mathrm{A/cm^2} \quad \textbf{(2)}$$

where i_{H_2O} is the cathodic current density for water reduction, F is Faraday's constant 96485 A/mol, E is the electrode potential in V with respect to the saturated calomel electrode, R is the molar gas constant 8.314 J mol^{-1} K^{-1}, T is the temperature of the test solution, 363 K for the current experiments.

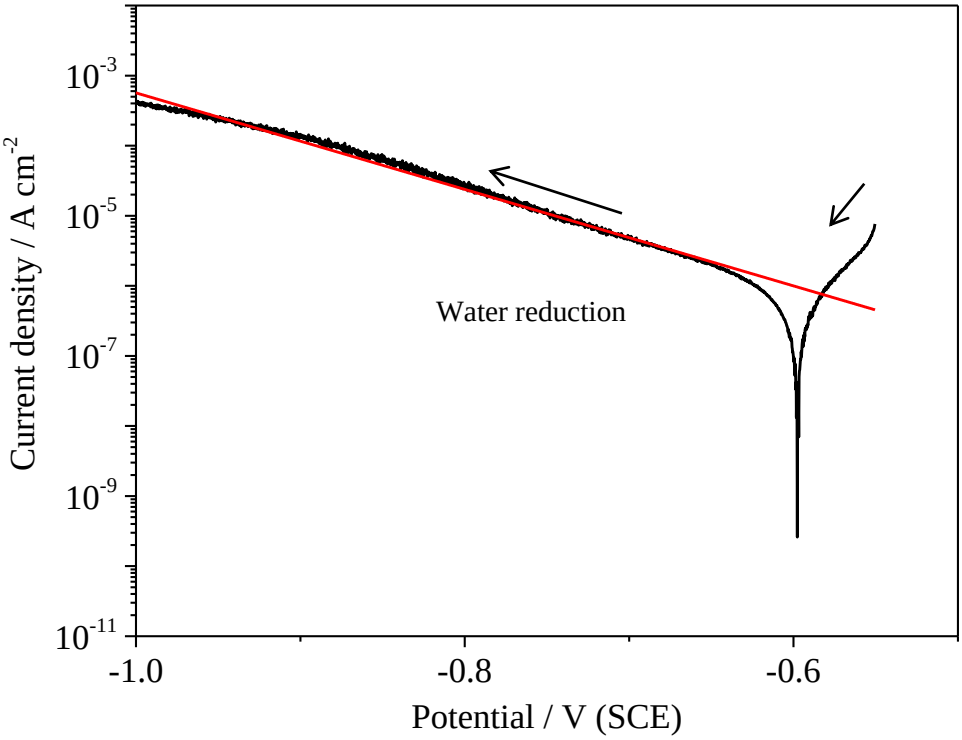

Figure 4: The potential of the specimen was swept from -550 mV (SCE) to -1000 mV (SCE) at a sweep rate of 1 mV/min in neutral solution containing 1000 ppm Cl^- at 90 °C. The specimen was immersed in the deaerated solution for eleven days before the sweep. A fitted line (in red) according to Equation (2) is also plotted.

3.3 HYDROGEN ION REDUCTION KINETICS IN DEAERATED ACIDIC SOLUTIONS CONTAINING 1000 PPM Cl^- AT 90 °C

Figure 5 shows the cathodic polarisation curves of three specimens immersed in acidic solutions (containing 1000 ppm Cl^-) of pH 2.2, 3.1 and 4.0. In the low pH regime in Figure 5, hydrogen ion reduction was the dominant cathodic reaction. Hydrogen ion reduction occurs as follows:

$$2H^+ + 2e^- \rightarrow H_2 \qquad \textbf{(3)}$$

A linear cathodic Tafel region is required to obtain the hydrogen ion reduction kinetics. However, generating reliable data in this environment is not so straightforward. The passive current should be low to minimise the impact on the net current; mass transport should be maximised to minimise diffusion limited reduction and extend the Tafel region; and the conductivity should be low to minimise the potential drop at high current densities.

When the cathodic overpotential is low (near OCP), both anodic and cathodic current contribute to the net current measured. Accordingly, before cathodic polarization, the specimen was held at either -290 mV (SCE) or -300 mV (SCE) for a period of time for the growth of the protective passive layer to decrease the anodic passive current density to a sufficiently low level. The anodic passive current density increased with decreasing pH for the solutions used (pH 2.2, 3.1 and 4.0). Consequently, solutions with a high value of pH are favoured in that respect.

During the cathodic polarisation, the current increased exponentially with the potential where the hydrogen ion reduction kinetics can be determined but mass transport limitations ensued. Furthermore, at progressively more negative potentials the polarisation curve deviated from the linear region on the log plot with increasing current due to the increased potential drop across the solution and electrodes. The potential drop is expected to be lower in a more acidic solution than a less acidic one since the conductivity of a more acidic solution is greater than that of a less acidic one but the current is higher and that counteracts any benefit.

As a result, a reasonable cathodic Tafel region was observed only in the solution with pH 3.1 where there were comparatively low anodic passive current densities at low cathodic overpotential and small potential drop when the cathodic current density was high. These data were therefore used to determine the Tafel slope and the transfer coefficient.

The reaction order with respect to the hydrogen ion concentration was estimated as:

$$\frac{\partial \log(i_{H^+})}{\partial \log([\mathrm{H}^+])} \approx 2 \qquad \textbf{(4)}$$

where i_{H^+} is the cathodic current density for hydrogen ion reduction and [H^+] is the hydrogen ion concentration, in mol/L.

According to the data in Figure 5, the hydrogen ion reduction kinetics can be represented by:

$$i_{H^+} = 4.2 \times 10^{-8}[\mathrm{H}^+]^2 \exp\left[-\frac{1.5\mathrm{F}E}{\mathrm{R}T}\right] A/cm^2 \qquad \textbf{(5)}$$

Fitted lines using Equation (5) are shown in Figure 5 and are in good agreement with the experimental results within the limitations indicated above.

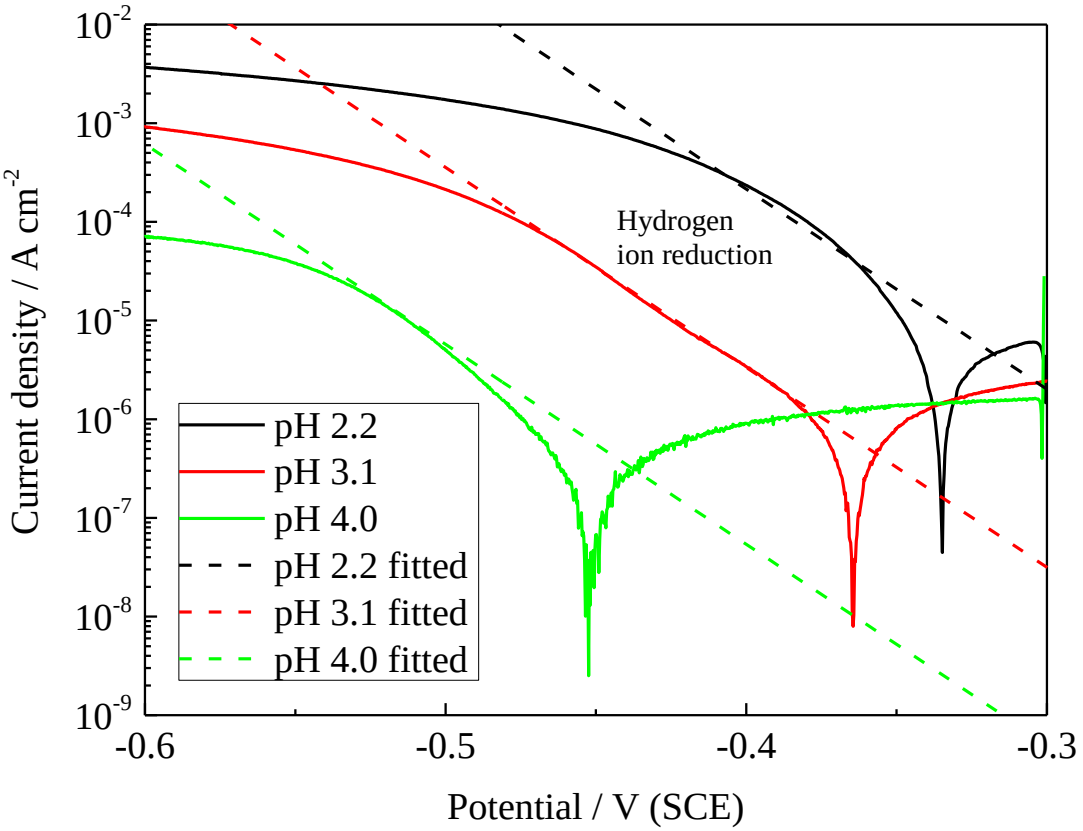

Figure 5: Specimens were held at -290 mV (SCE) or -300 mV (SCE) for 6 hours (pH 2.2), 72 hours (pH 3.1) and 70 hours (pH 4.0) and then a potential sweep started from -290 mV (SCE) or -300 mV (SCE) to the cathodic region at 1 mV/min. Specimens were immersed in solutions of 1000 ppm Cl^- with pH as indicated for one day (pH 2.2 and pH 4) and three days (pH 3.1) before the potentiostatic and the sweep test. Fitted lines according to Equation (5) are also plotted.

The observed transfer coefficient: 1.5 is ascribed to the following steps in the hydrogen ion reduction reaction [11-13]:

$$H^+ + e^- \overset{\text{fast}}{\Leftrightarrow} H_{ads} \quad \textbf{(6)}$$

$$H^+ + H_{ads} + e^- \overset{\text{slow}}{\longrightarrow} H_2 \quad \textbf{(7)}$$

i.e. fast discharge (Volmer reactions) and slow electrochemical recombination (Heyrovsky reactions), the latter being rate-determining. This is consistent also with the reaction order dependence of the current density on hydrogen ion concentration.

3.4 DEPASSIVATION pH

Potentiodynamic tests were carried out in a series of solutions with pH ranging from 4.0 to 1.7 to investigate the critical pH for depassivation, at which the transition from passive to predominantly active corrosion takes place [14-16].

Figure 6 shows the polarisation curves of the specimen polarised from OCP to the anodic region. It can be observed that for solutions with pH 1.9 to 4.0, the current density was nearly independent of the potential when the potential was 50–100 mV above OCP. This indicated that the specimen was in the passive state. The passive current density of the specimen in solutions with pH values varying from 2.3

to 4.0 was in the range of 10^{-6}–10^{-5} A/cm^2 but increased to 10^{-5}–10^{-4} A/cm^2 for solutions with pH 1.9 or 2.1. Note that there was a big jump in passive current density from pH 2.8 to pH 2.6. For the specimen in solutions with pH 1.7, the current density kept increasing with increasing potential, which indicated active dissolution of the metal. The test was stopped when the current density was greater than 2 mA/cm^2. Examination of the surface after testing suggested incomplete deactivation, with the surface exhibiting a high density of corrosion pits, which could be the precursor to more general attack. Since the passive to active state usually occurs by initial attack at inclusion sites it can be difficult to distinguish in short term tests whether this is truly depassivation or simply extended pitting. Nevertheless, we will refer to that pH as the depassivation pH.

The results indicate that the depassivation pH of FV566 is between 1.7 and 1.9. It should be noted that at pH 1.7, the chloride ion concentration of the solution had increased to 2120 ppm due to the addition of hydrochloric acid, as shown in Table 2. The increased chloride ion concentration might have an effect on the value of depassivation pH. Marcelin [17] reported that when the chloride ion concentration was greater than 0.8 ± 0.2 M (~2.9 × 10^4 ppm), the martensitic stainless steel studied was in the active state and dissolution occurred. However, Narasi and his co-workers [16] have measured the depassivation pH of alloy 825 in deaerated solutions with chloride ion concentration varying from 0.5 M to 4 M (~0.2–1.4 × 10^5 ppm) at 95 °C, suggesting that the depassivation pH was independent of chloride ion concentration.

As demonstrated in Section 3.1, the passive current density of the specimen in neutral solutions decreased with increasing exposure time, indicating that the specimen became less active with greater exposure time. Consequently, if the material is exposed for a much longer time in real applications than the current study (immersion time in the current study was limited by the experimental method used), the depassivation pH determined in the current study might overestimate the critical value that would be expected in reality, i.e., the critical value determined here is a conservative value.

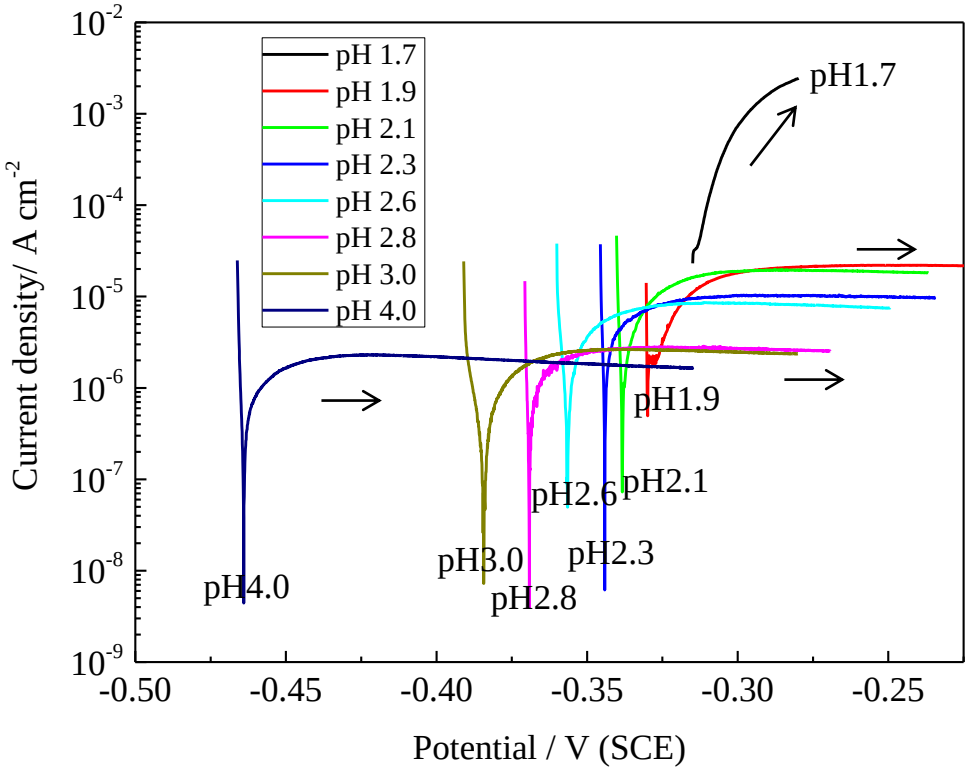

Figure 6: Specimens were polarised from OCP to the anodic region at 1 mV/min. Tests were carried out in solutions at 90 °C with the value of pH indicated in the diagram and the corresponding chloride ion concentration shown in Table 2. Immersion time of specimens in solutions at OCP before sweep tests was: 3 days for pH 4 and pH 3; 4 days for pH 2.8; 5 days for pH 2.6 and pH 2.3; 6 days for pH 2.1 and pH 1.9 and 7 days for pH 1.7.

4 CONCLUSIONS

Electrochemical data were generated as input to the crack chemistry model being developed to understand the factors controlling the crack growth rate in steam turbine blade steel.

- The passive current density of FV566 in deaerated neutral solutions containing 1000 ppm Cl^- was measured. It was shown that the test method affected the values of the passive current density. In the potentiodynamic tests, the passive current density was 3.0–6.5 μA/cm^2 with a sweep rate of 10 mV/min and 0.6-3.1 μA/cm^2 with a sweep rate of 1 mV/min. In the potentiostatic tests, the passive current density of the specimen was 0.07 μA/cm^2 after holding the specimen at -300 mV (SCE) for 116 hours. The difference in the value of passive current densities was attributed to the different immersion time. The longer immersion time might lead to a thicker/denser passive layer and consequently a lower passive current density.

- Potentiodynamic tests were carried out to investigate the water reduction kinetics of FV566 in deaerated neutral solutions containing 1000 ppm Cl^- at 90 °C. The water reduction kinetics could be represented by:

$$i_{H_2O} = 2.9 \times 10^{-11} \exp\left(-\frac{0.54\mathrm{F}E}{\mathrm{R}T}\right) A/cm^2$$

- Potentiodynamic tests were carried out in deaerated acidic solutions (at pH: 2.2, 3.1 and 4.0) containing 1000 ppm Cl^- at 90 °C to study the hydrogen ion reduction kinetics of FV566. The hydrogen ion reduction kinetics could be represented (with $[H^+]$ specified in mol/L) by :

$$i_{H^+} = 4.2 \times 10^{-8}[\mathrm{H}^+]^2 \exp\left[-\frac{1.5\mathrm{F}E}{\mathrm{R}T}\right] A/cm^2$$

- The depassivation pH, at which the transition from passive to active corrosion takes place, was determined by polarising the specimen from OCP to the anodic region in deaerated solution. For solutions with pH values not lower than 1.9, the specimen was still in passive region when the potential was at least 100 mV above OCP. For the solution with a pH value of 1.7 no passive region was observed and the current kept increasing from the OCP with increasing potential. Consequently, the depassivation pH of FV566 in deaerated solutions containing ~2000 ppm Cl^- at 90 °C is deduced to lie between 1.7 and 1.9. However, this is expected to be a conservative value compared with real applications.

ACKNOWLEDGEMENTS

This work was conducted as part of a joint venture between the United Kingdom Department for Business, Energy and Industrial Strategy (BEIS) and an industrial group comprising S. Fenton (Uniper Technologies Limited, UK), D. Gass (Siemens), W. Hahn (EDF Energy), H. Pitts (HSL), S. Osgerby (GE Power), P. Reed (U. Southampton) and A. Rowe (RWE npower).

REFERENCES

[1] A. Turnbull, The environmentally small/short crack growth effect: current understanding, Corros. Rev., 30 (2012) 1-17.
[2] S. Zhou, M. Lukaszewicz, A. Turnbull, Small and short crack growth and the solution-conductivity dependent electrochemical crack size effect, Corros. Sci., 97 (2015) 25-37.
[3] A. Turnbull, S. Zhou, M. Lukaszewicz, An approach to measurement of environmentally assisted small crack growth, Corrosion, Orlando, USA, NACE International, 2013.
[4] A. Turnbull, S. Zhou, M. Lukaszewicz, Environmentally Assisted Small Crack Growth, Procedia. Materials Science, 3 (2014) 204-8.

[5] A. Turnbull, S. Zhou, Electrochemical short crack effect in environmentally assisted cracking of a steam turbine blade steel, Corros. Sci, 58 (2012) 33-40.
[6] W.M. Hyanes, D.R. Lide, in CRC Handbook of Chemistry and Physics, 92nd ed 2011-2012.
[7] C.O.A. Olsson, D. Landolt, Passive films on stainless steels - chemistry, structure and growth, Electrochim. Acta, 48 (2003) 1093-104.
[8] C.M. Abreu, M.J. Cristobal, R. Losada, X.R. Novoa, G. Pena, M.C. Perez, Long-term behaviour of AISI 304L passive layer in chloride containing medium, Electrochim. Acta, 51 (2006) 1881-90.
[9] J.J. Kim, Y.M. Young, Study on the Passive Film of Type 316 Stainless Steel, Int. J. Electrochem. Sci., 8 (2013) 11847-59.
[10] A. Turnbull, Impact of graphite gasket duplex stainless steel couples on crevice chemistry and the likelihood of crevice attack in seawater, Corrosion, 55 (1999) 206-12.
[11] R.G. Compton, C.E. Banks, in Understanding of Voltammetry, World Scientific Publishing Co. Pte. Ltd., 2007.
[12] J. McBreen, M.A. Genshaw, The electrochemical introduction of hydrogen into metals Fundamental Aspects of Stress Corrosion Cracking, in Fundamental aspects of stress corrosion cracking, Naitonal Association of Corrosion Engineers, 1969.
[13] N. Ohnaka, Y. Furutani, Electrochemical Investigation of Hydrogen Absorption of Type 304 Stainless Steel in 0.05 M Na2SO4 Solutions of Different pH at 95°C, Corrosion, 46 (1990) 129-35.
[14] H. Ogawa, K. Denpo, A. Miyasaka, Criteria for passivity breakdown of high alloy materials in relation to crevice corrosion nucleation, Corros. Sci., 31 (1990) 459-64.
[15] S. Azuma, H. Miyuki, T. Kudo, Effect of alloying nitrogen on crevice corrosion of austenitic stainless steels, ISIJ Int., 36 (1996) 793-8.
[16] S. Narasi, G.A. Cragnolino, Applicability of repassivation potential for long-term prediction of localized corrosion of Alloy 825 and type 316L stainless steel, Corrosion, 49 (1993) 885-94.
[17] S. Marcelin, N. Pebere, S. Regnier, Electrochemical investigations on crevice corrosion of a martensitic stainless steel in a thin-layer cell, Journal of Electroanalytical Chemistry, 737 (2015) 198-205.